

Restoration of tensile properties in cracked aluminum specimens via composite patching**Touam Lakhemissi^a, Rebai Billel^{a*}, Derfouf Semcheddine^{b,c} and Messas Tidjani^a**^aFaculty of Sciences & Technology, Civil Eng Department, University Abbes Laghrou Khenchela, Algeria^bFaculty of Technological Sciences, University of Batna 2, 05078 Batna, Algeria^cLGM Mechanical Engineering Laboratory Biskra University, BP 145, Biskra 07000, Algeria**ARTICLE INFO***Article history:*

Received 2 October 2023

Accepted 16 January 2024

Available online

16 January 2024

*Keywords:**Composite materials**Tensile testing**Aluminum; repair**Fiberglass**Laminates***ABSTRACT**

This study investigates the tensile behavior and crack repair of aluminum using fiberglass-reinforced composite patches. Tensile testing compared uncracked, pre-cracked, and repaired aluminum specimens. Pre-cracking by hole drilling decreased strength and ductility from stress concentrations. Composite patching recovered strength, with 4-ply laminates optimal. Uncracked samples failed by necking, pre-cracked by crack growth, and repaired by adhesive detachment. Results demonstrate composite patching effectively restores strength to cracked aluminum by mitigating stress concentrations when appropriately designed. Finite element modeling simulated stress reduction after patching. This work provides experimental data on composite patch performance for metal crack repair and confirms the approach as an effective strengthening technique, although further optimization is needed.

1. Introduction

The pervasive integration of composite materials in the rehabilitation and fortification of fissured metallic structures has become increasingly pronounced across diverse sectors, including aerospace, infrastructure, and transportation (Shinde et al., 2020; Berkia et al., 2023; Billel, 2023; Billel, 2022; Rebai et al., 2023). Noteworthy attributes such as corrosion resistance, a superior strength-to-weight ratio, and adaptability in design render composites particularly well-suited for the adhesive repair of impaired metallic components. Commonly employed in this context are fiber-reinforced polymer composites, featuring fibers such as glass, carbon, and aramid embedded within polymer matrices, with the composite patch affixed to the damaged structure through the application of structural adhesives.

The restoration of tensile properties in fissured aluminum specimens can be achieved through the judicious implementation of composite patching. Several investigations have been conducted to assess the efficacy of composite patches in rectifying cracked aluminum plates. Dindar and Ağır (2021) undertook a study utilizing E-glass/epoxy composites for patching aluminum plates exhibiting 'O' and 'U' notches. Hart and Bruck (2021) delved into the impact of low modulus composite patch repairs on crack tip plasticity and strain energy release rate in metallic plates. Dehuri and Pradhan (2020) scrutinized the correlations between Rockwell hardness and tensile strength in cracked aluminum plates repaired with composite patches. Abd-Elhady et al. (2021) investigated the mitigating effects of bonded carbon fiber-reinforced polymer (CFRP) patches on reducing crack tip driving force. Yousefi et al. (2021) analytically probed the fatigue behavior of aluminum alloy, subject to repair by a double-sided glass/epoxy composite patch, revealing substantial enhancements in fatigue life. Collectively, these studies underscore the potential of composite patching as an efficacious method for reinstating tensile properties in fractured aluminum specimens.

The efficacy of composite patching in rectifying fractured aluminum specimens has been substantiated through a diverse

* Corresponding author.

E-mail addresses: billel.rebai@univ-khenchela.dz (R. Billel)

array of research endeavors. The utilization of low modulus composite patches has been shown to notably augment crack tip plastic strain, thereby contributing to enhanced failure prediction methodologies, as explored by Hart and Bruck (2020). Dai et al. (2020) conducted an examination of glass fiber-reinforced polymer (GFRP) materials, demonstrating their commendable efficiency in repairing cracked aluminum plates and effecting strength recovery. Makwana and Shaikh (2019) proposed hybrid composite patches, amalgamating carbon fiber and glass fiber, as an economical repair solution for fractured aluminum panels, exhibiting adequate performance in mitigating stress intensity and managing interfacial stresses. Dehghanpour et al. (2019) explored diffusion bonding as a reparative technique, yielding promising outcomes in terms of maximum tensile strength and force tolerance. Furthermore, Bianchi et al. (2019) conducted investigations into the application of composite patching for underwater structures, revealing robust interface strength and manifesting potential for successful structural restoration.

Innovatively, composite patches incorporating prestressed Nitinol shape memory alloy (Ni-Ti SMA) wires have emerged as a viable strategy for repairing fractured aluminum sheets. The incorporation of SMA wires within these patches has been demonstrated to reduce the stiffness ratio, subsequently diminishing the J-integral and plastic area dimensions in comparison to patches devoid of SMA wires, as evidenced by Nejati et al. (2023). An alternative approach to mending fractured aluminum sheets involves the use of Carbon Fiber Reinforced Plastics (CFRP) patches, as elucidated by Kadam et al. (2023). Numerical simulations conducted by Ahmed et al. (2022) have indicated that augmenting the length of the CFRP patch significantly mitigates the stress intensity factor (SIF) range, thereby enhancing the fatigue life of the rehabilitated aluminum panel. Remarkably, the performance of a repair employing a bonded CFRP patch rivals that achieved by an aluminum alloy patch affixed through riveting, as reported by Lokhande et al. (2023).

In this study, an examination is undertaken to scrutinize the tensile behavior and crack remediation of aluminum specimens through the application of fiberglass-reinforced composite patches. Aluminum alloys, constituting crucial structural materials in diverse applications, are susceptible to cracks and damage during manufacturing or service, necessitating reparative interventions to reinstate mechanical integrity. The efficacy of composite repair is contingent upon various factors, encompassing patch material and design, surface preparation, and adhesive selection. Employing experimental tensile testing facilitates a quantitative assessment of composite patching.

The primary objective of this research is to meticulously analyze and juxtapose the tensile properties of uncracked aluminum, pre-cracked samples, and repaired specimens. Such an analysis aims to unveil the ramifications of cracking on tensile performance and elucidate the restorative capabilities of composite patches in recovering mechanical properties. Furthermore, an investigation into the influence of patch parameters, including the number of layers and material composition, is conducted. The comprehensive presentation of testing methodology, results, and analytical insights is proffered.

This inquiry critically assesses the effectiveness of fiberglass composite repair for cracked aluminum, contributing valuable empirical data on composite patch performance. The acquired insights are poised to inform the design of reparative strategies, thus enhancing the understanding and application of composite patches in the context of cracked aluminum structures.

2. Test materials and methods

The process of selecting materials for composite patch repair entails the careful consideration of suitable reinforcement and adhesive options. Traditionally, fiberglass fabrics have been widely favored as a reinforcement choice owing to their favorable mechanical attributes and cost-effectiveness. In the context of this study, we have opted for fiberglass fabric and mat as the primary patch materials.

The adhesive component holds a pivotal role in ensuring the success of the repair process. Factors such as viscosity, working life, curing temperature, and bond strength are crucial considerations during the adhesive selection phase. Extensive testing has been conducted to compare various adhesives, with the objective of identifying the most optimal one for the specific application at hand. In this research, epoxy resin has been chosen as the adhesive due to its commendable mechanical properties post-curing and its effectiveness in bonding the patch to the metal substrate.

Table 1 and **Table 2** encapsulate a comprehensive summary of the key properties associated with the selected epoxy adhesive, both in its non-cured and cured states. It is imperative to underscore that the judicious selection of both reinforcement and adhesive components is essential for attaining the requisite mechanical performance in composite repairs.

Table 1. Non-polymerized properties of the adhesive

Property	Values
Chemical Base	Epoxy Resin
Appearance	Clear/Transparent
Density	1.15
Temperature Range	-35 to 800 °c
Mixing Ratio	1 : 1

Table 2. Polymerized properties of the adhesive

Property	Values
Pot Life (Workable Time)	5 minutes
Final Strength	8 heures
Shear Strength	58 MPa
Tensile Strength	40 MPa
Peel Strength	9 MPa

2.1 Specimens used

The specimens used in the experiments are flat aluminum plates with a thickness of 3 mm. Several different sample types have been tested:

- **Uncracked Samples:** These are used to determine the baseline mechanical properties of the aluminum material.
- **Cracked Samples:** Holes of 2 mm, 3 mm, and 4 mm in diameter have been drilled in the center of the samples to artificially induce cracks. This is depicted in **Fig. 1** and **Fig. 2**.
- **Repaired Samples:** Cracked samples have been repaired by bonding composite patches over the holes. The patches are made of fiberglass fabric or mat in 4-ply laminates.

The number of repaired samples matches the number of pre-cracked samples for each hole diameter.

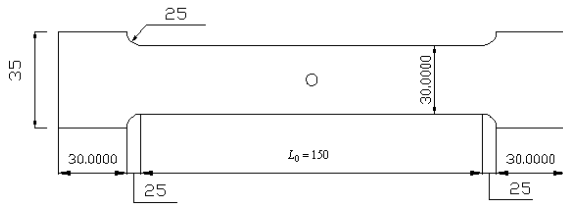


Fig. 1. Unidirectional plate specimen size chart (Unit: mm)

Fig. 2. Specimens pierced with diameters (1-2-3-4) mm

2.2 Composite Material Application Process

The first layer of fabric (mat) is applied directly on the adhesive already applied on the surface of the plate; the other layers are glued on top of each other above the first layer. (**Fig. 3** and **Fig. 4**.)

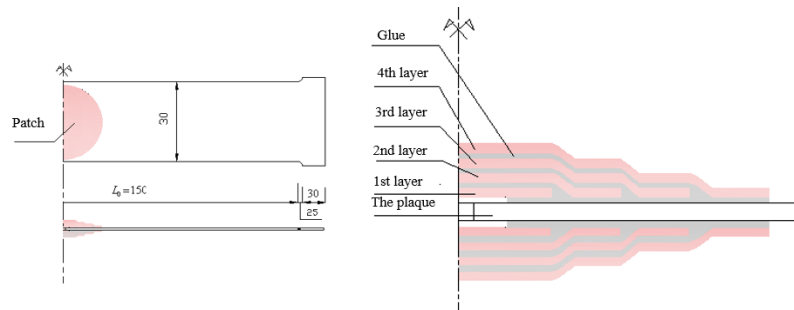
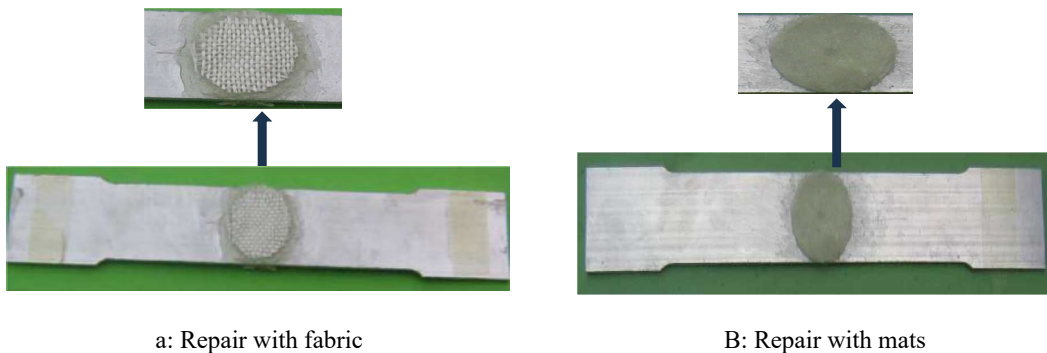


Fig. 3. Geometry of the repaired specimen



a: Repair with fabric

B: Repair with mats

Fig. 4. Repair of specimens

Fig. 5 shows a specimen mounted in the testing apparatus. Tensile testing is being performed on samples of each type. Mechanical properties, including strength, breaking force, and deformation, are being measured. Stress-strain curves are being generated for analysis and comparison of the different sample conditions.



Fig. 5. View of the Specimen Positioned Between the Machine's jaws

3. Test results and analysis

This section presents and deliberates on the outcomes of the tensile tests conducted on uncracked, pre-cracked, and repaired aluminum samples. The primary objective has been to assess the efficacy of employing composite patching to restore strength in structures afflicted with cracks.

Uncracked testing has established the baseline mechanical properties of the aluminum. Introducing pre-cracks through drilling has led to diminished strength, force, and ductility, attributed to stress concentrations. Repaired samples involved the application of 4-ply fiberglass laminate patches affixed over the drilled holes. Results indicate a notable recovery in strength and performance for the repaired samples when compared to their cracked counterparts. The optimal configuration involved either 2 fabric layers or 3 mat layers.

Failure modes observed included necking in uncracked samples, crack propagation in pre-cracked ones, and adhesive detachment in the repaired specimens. In summary, the tensile tests unequivocally demonstrate the advantageous effects of composite repair in ameliorating degradation caused by cracks. This is achieved by mitigating stress concentrations when the repair is appropriately designed and applied.

3.1 Tensile test on smooth specimens.

This section offers a comprehensive examination of the mechanical properties of various specimens, taking into account different diameters and repair techniques. These properties play a vital role in evaluating the material's performance and structural integrity across varying conditions. The figures and tables are sequentially labeled from **Table 4** to **Table 9** and encompass stress-strain curves (**Figs. 6-12**) from tensile test data, providing information on longitudinal elasticity module (E), conventional proportional limit, ultimate tensile strength (Rm), percentage elongation at rupture (A), and the coefficient of contraction (Z). A collective analysis of these tables allows us to discern the influence of specimen diameter and repair methods on the material's mechanical behavior.

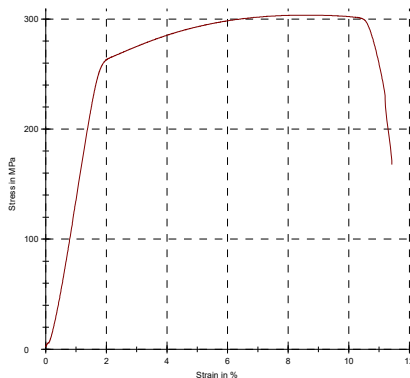


Fig. 6. Stress-strain curve in a tensile test on the smooth specimen

Table 3. Mechanical properties of the smooth specimen

E: Longitudinal Elasticity Module	16,59	GPa
Conventional Proportional Limit	262	MPa
Rm: Mechanical Strength (Tensile Strength)	304	MPa
A: Percentage Elongation at Rupture	10,2	%
A: Percentage Elongation at Rupture (Manual)	9,29	%
Z: Contraction Coefficient	51,0	%

3.2 Tensile test on pierced and fabric laminate repaired specimens

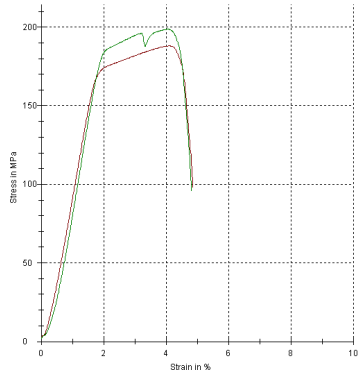


Fig. 7. Stress-strain curve in a tensile test

Table 4. Mechanical properties of the 2mm diameter pierced specimen and the fabric repaired specimen

	Pierced specimen (brown)	Repaired specimen (green)	
E: Longitudinal Elasticity Module	11,14	11,85	GPa
Conventional Proportional Limit	173	186	MPa
Rm: Mechanical Strength (Tensile Strength)	188	199	MPa
A: Percentage Elongation at Rupture	3,8	3,7	%
A: Percentage Elongation at Rupture (Manual)	5	4,29	%
Z: Contraction Coefficient	67,7	65,8	%

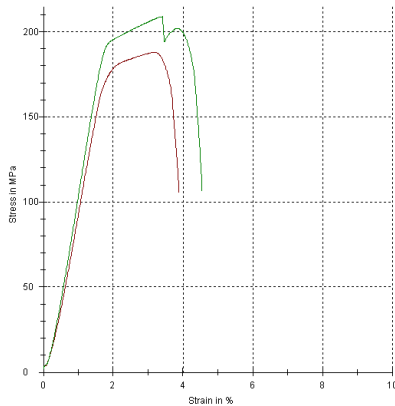


Fig. 8. Stress-strain curve in a tensile test

Table 5. Mechanical properties of the 3mm diameter pierced specimen and the fabric repaired specimen

	Pierced specimen (brown)	Repaired specimen (green)	
E: Longitudinal Elasticity Module	11,43	12,66	GPa
Conventional Proportional Limit	177	194	MPa
Rm: Mechanical Strength (Tensile Strength)	188	209	MPa
A: Percentage Elongation at Rupture	2,8	3,5	%
A: Percentage Elongation at Rupture (Manual)	4,29	5	%
Z: Contraction Coefficient	67,9	65,7	%

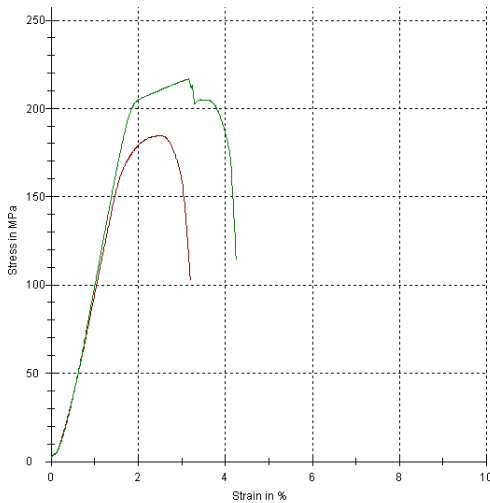


Fig. 9. Stress-strain curve in a tensile test

Table 6. Mechanical properties of the 4mm diameter pierced specimen and the fabric repaired specimen

	Pierced specimen (brown)	Repaired specimen (green)	unit
E: Longitudinal Elasticity Module	11,92	13,12	GPa
Conventional Proportional Limit	175	205	MPa
Rm: Mechanical Strength (Tensile Strength)	185	217	MPa
A: Percentage Elongation at Rupture	2,1	3,1	%
A: Percentage Elongation at Rupture (Manual)	2,86	3,57	%
Z: Contraction Coefficient	68	69,1	%

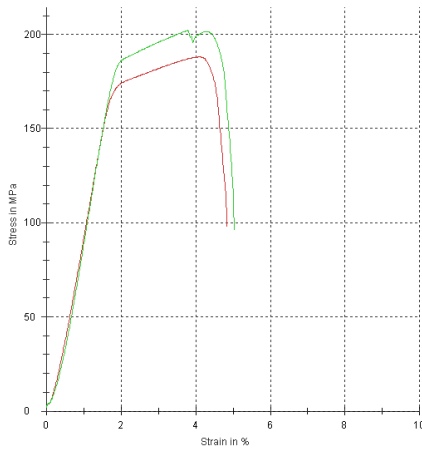


Fig 10. Stress-strain curve in a tensile

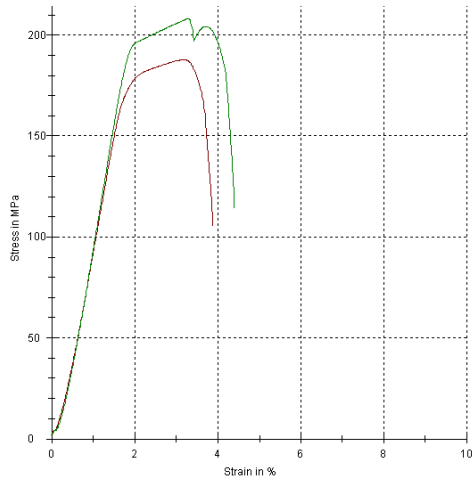


Fig. 11. Stress-strain curve in a tensile test

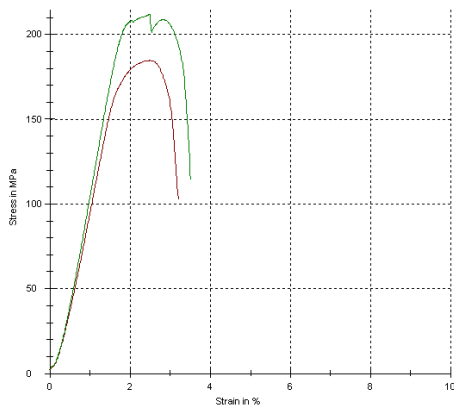


Fig. 12. Stress-strain curve in a tensile test

Table 7. Mechanical properties of the 2mm diameter pierced specimen and the mat laminate repaired specimen

	Pierced specimen (brown)	Repaired specimen (green)	Unit
E: Longitudinal Elasticity Module	11,14	11,5	GPa
Conventional Proportional Limit	173	187	MPa
Rm: Mechanical Strength (Tensile Strength)	188	202	MPa
A: Percentage Elongation at Rupture	3,8	4	%
A: Percentage Elongation at Rupture (Manual)	5	4,29	%
Z: Contraction Coefficient	67,7	65,5	%

Table 8. Mechanical properties of the 3mm diameter pierced specimen and the mat laminate repaired specimen

	Pierced specimen	Repaired specimen	Unit
E: Longitudinal Elasticity Module	11,43	12,29	GPa
Conventional Proportional Limit	177	196	MPa
Rm: Mechanical Strength (Tensile Strength)	188	208	MPa
A: Percentage Elongation at Rupture	2,8	3,2	%
A: Percentage Elongation at Rupture (Manual)	4,29	3,86	%
Z: Contraction Coefficient	67,9	69,2	%

Table 9. Mechanical properties of the 4mm diameter pierced specimen and the mat laminate repaired specimen

	Pierced specimen (brown)	Repaired specimen (green)	Unit
E: Longitudinal Elasticity Module	7	14	GPa
Conventional Proportional Limit	11,92	13,12	MPa
Rm: Mechanical Strength (Tensile Strength)	175	205	MPa
A: Percentage Elongation at Rupture	13438	14651	%
A: Percentage Elongation at Rupture (Manual)	2,1	3,1	%
Z: Contraction Coefficient	2,86	3,57	%

Analysis of the mechanical properties reveals several salient trends. The modulus of longitudinal elasticity (E) increases with larger specimen diameters, with repaired specimens exhibiting higher E values than pierced specimens; mat laminate repaired specimens displayed the highest E . Similarly, conventional proportional limits rose with increasing specimen diameter, with repaired specimens having higher limits than pierced types, and mat laminate repaired specimens showing the highest values. The ultimate tensile strength (R_m) also increased with larger diameters, following the same pattern of repaired specimens outperforming pierced ones, and mat laminate repaired specimens demonstrating the highest R_m . In contrast, the percentage elongation at rupture (A) decreased with larger diameters for both pierced and repaired specimens, with repairs potentially having slightly lower A values. The coefficient of contraction (Z) showed greater variability without clear diameter or repair type trends. In summary, key mechanical properties including E , proportional limit, and R_m improved with larger diameters and repaired versus pierced specimens, particularly mat laminate repairs displaying the highest values. Elongation at rupture decreased with diameter, while contraction coefficient was more variable. These findings elucidate the influences of specimen diameter and repair type on mechanical behavior.

3.4 Failure modes of the specimens

Fig. 13 offers a comprehensive exploration of the failure modes observed within the tested specimens, providing crucial insights into their structural behavior. As we delve into this analysis,

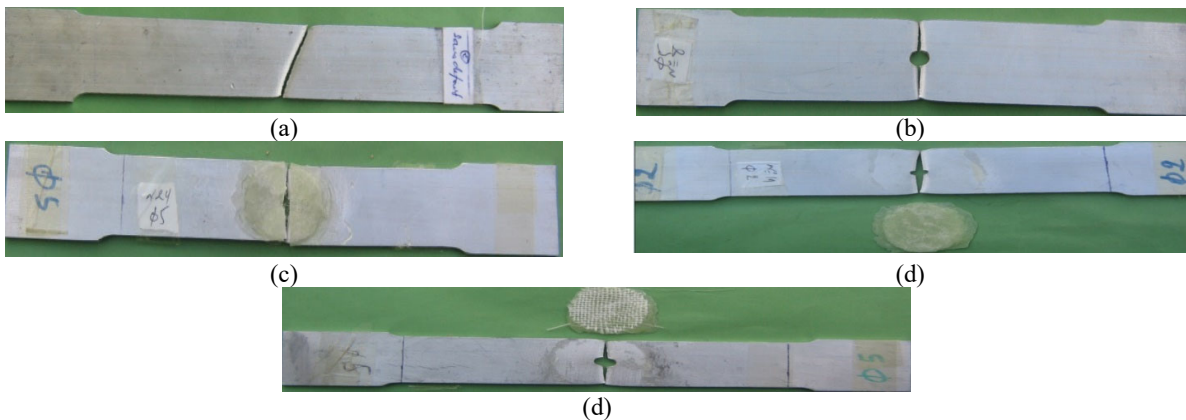


Fig 13. Illustration of the failure modes of the tested specimens.

Examination of the failure modes reveals several key insights. **Fig. 13(a)** and **Fig. 13(b)** illustrate the necking behavior in healthy and mid-pierced specimens, with the perforated specimens exhibiting symmetric versus asymmetric failure for non-pierced. Notably, all mid-pierced specimens showed consistent failure at the hole, underscoring its influence. In contrast, **Fig. 13(c)** demonstrates laminate failure with three mat layers, with the intact adhesive highlighting laminate stress absorption. However, **Fig. 13(d)** shows adhesive failure with four mat layers, leaving the laminate unaffected. **Fig. 13(e)** reveals another mode - adhesive failure despite intact laminate - more prominent with four fabric layers. Clearly, layer number delineates laminate and adhesive strength relationships; more layers impart greater laminate strength than the adhesive, while less than three layers result in stronger adhesive. In summary, these findings elucidate the structural behaviors of these composite materials under varying conditions, with failure modes dependent on factors including hole presence, layer number, and relative laminate/adhesive strength.

In the next section; Numerical simulations were conducted to investigate composite patch repair of cracked structures using the Castem finite element code. The aim was to model elimination of crack tip stress concentrations before and after repair. The repair process was modeled using Castem software on a plate containing a hole representing the crack. A 4-layer fiberglass patch bonded over the hole was simulated. Identical loading conditions were modeled before and after the simulated repair to enable comparisons.

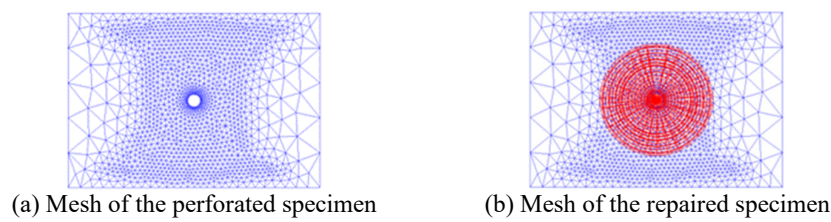


Fig. 14. Meshes of the specimens

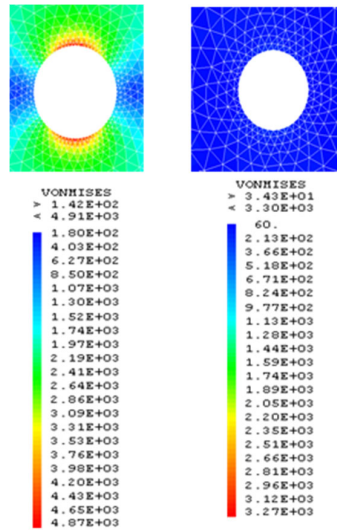
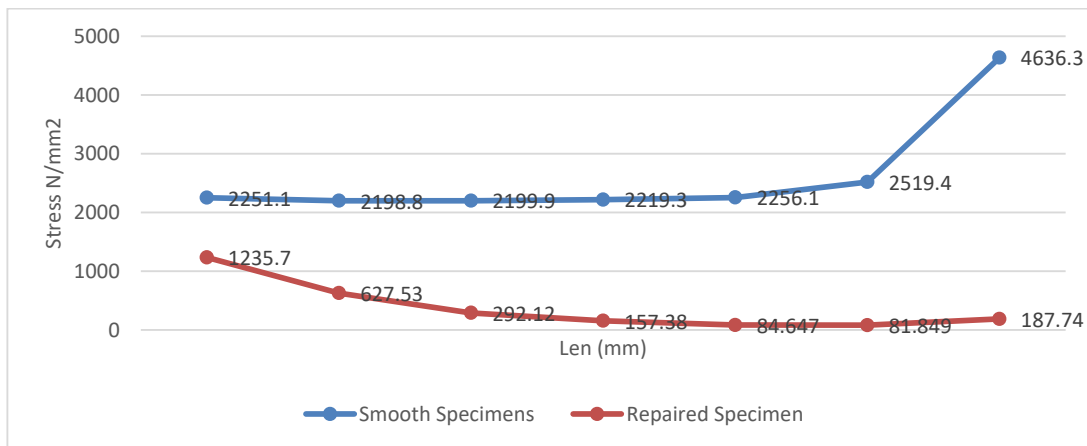


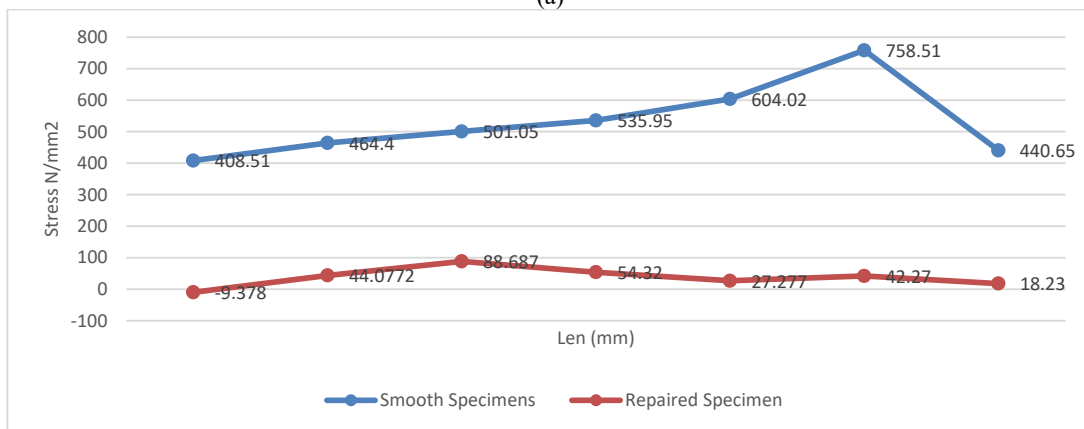
Fig. 15. Visualization of stresses in the perforated plate before and after repair

Numerical simulations were conducted to investigate composite patch repair of cracked structures using the Castem finite element code. The aim was to model elimination of crack tip stress concentrations before and after repair.

The repair process was modeled using Castem software on a plate containing a hole representing the crack. A 4-layer fiberglass patch bonded over the hole was simulated. Identical loading conditions were modeled before and after the simulated repair to enable comparisons.



(a)



(b)

Fig 16. Stress evolution before and after repair from the edge of the plate to the hole (along line L)

The stress evolution along line L (**Fig. 16**) elucidates a substantial decrease in stresses after laminate bonding, particularly at the hole edge where a stress concentration previously existed.

4. Conclusions

Experimental tensile testing revealed degraded mechanical properties including strength, elongation, and proportional limit in pre-cracked aluminum specimens versus uncracked material. Repairing holes with 4-ply fiberglass laminate patches recovered tensile performance to varying degrees depending on patch material; fabric repairs provided superior property enhancement over mat laminate for larger holes. Testing and analysis clearly demonstrated effective strength restoration in cracked metallic structures via properly designed composite repairs, mitigating stress concentration effects. However, further optimization of patch design is warranted. Numerical simulations using Castem finite elements modeled elimination of crack tip stress concentrations before and after repair, elucidating the repair process. In summary, composite patching was shown to be an effective repair technique for cracked aluminum, recovering mechanical performance, although additional work is needed on optimizing patch design and materials.

References

- Abd-Elhady, A. A., Mousa, S., Alhazmi, W. H., Sallam, H. E. M., & Atta, M. (2021). Effects of composite patching on cyclic crack tip deformation of cracked pinned metallic joints. *The Journal of Adhesion*, 97(16), 1561-1577.
- Ahmed, F., Mohammed, S. M. A. K., Benyahia, F., Bouiadjra, B. A. B., & Albedah, A. (2022, December). Plasticity Analysis in Aluminum Alloy Plates Repaired with Bonded Composite Patch Under Overload. *In Proceedings of the 10th International Conference on Fracture Fatigue and Wear: FFW 2022*, 2-3 August, Ghent University, Belgium (pp. 21-27). Singapore: Springer Nature Singapore.
- Berkia, A., Rebai, B., Litouche, B., Abbas, S., & Mansouri, K. (2023). Investigating parametric homogenization models for natural frequency of FGM nano beams. *AIMS Materials Science*, 10(5), 891-908.
- Bianchi, R. W., Kwon, Y. W., & Alley, E. S. (2019). Composite Patch Repair for Underwater Aluminum Structures. *Journal of Offshore Mechanics and Arctic Engineering*, 141(6), 064501.
- Billel, R. (2022, October). Effect of the Idealization Models and Thermal Loads on Deflection Behavior of Sandwich FGM Plate. *In 2022 International Conference on Electrical Engineering and Photonics (EExPolytech)* (pp. 260-264). IEEE.
- Billel, R. (2023). Contribution to study the effect of (Reuss, LRVE, Tamura) models on the axial and shear stress of sandwich FGM plate (Ti-6Al-4V/ZrO 2) subjected on linear and nonlinear thermal loads. *AIMS Materials Science*, 10(1).
- Dai, J., Zhao, P., Su, H., & Wang, Y. (2020). Mechanical behavior of single patch composite repaired al alloy plates: Experimental and numerical analysis. *Materials*, 13(12), 2740.
- Dehghanpour, S., Nezamabadi, A., Attar, M., Barati, F., & Tajdari, M. (2019). Repairing cracked aluminum plates by aluminum patch using diffusion method. *Journal of Mechanical Science and Technology*, 33, 4735-4743.
- Dehuri, B., & Pradhan, S. S. (2020). Correlations between hardness and tensile strength of cracked aluminium plates repaired with composite patches. *Materials Today: Proceedings*, 21, 1335-1339.
- Dindar, B., & Ağır, İ. (2021). Tensile and buckling properties of notched 6063 aluminum repaired with composite patches. *Emerging Materials Research*, 10(2), 139-144.
- Hart, D. C., & Bruck, H. A. (2020, November). Simplified method for predicting ultimate failure of one-sided composite patched aluminum center crack tension specimens. *In AIP Conference Proceedings* (Vol. 2309, No. 1). AIP Publishing.
- Hart, D. C., & Bruck, H. A. (2021). Predicting failure of cracked aluminum plates with one-sided composite patch. *International Journal of Fracture*, 227(2), 205-218.
- Kadam, S., Kumar, P., & Shinde, H. (2023). Repair of pre-cracked aluminium alloy panel with CFRP bonded patch and its comparison with riveted patch. *Materials Today: Proceedings*, 72, 1190-1196.
- Lokhande, M., Shinde, P. S., Kumar, P., & Shinde, H. P. (2023). Fatigue life of thin pre-cracked aluminum alloy panel repaired with CFRP patch at elevated temperature. *Materials journal*, 72, 1869-1876.
- Makwana, A. H., & Shaikh, A. A. (2019). Towards hybridization of composite patch in repair of cracked Aluminum panel: numerical and experimental study. *International Journal of Structural Integrity*, 10(6), 868-887.
- Nejati, M., Shokrieh, M. M., & Ghasemi Ghalebahman, A. (2023). Reinforcement of cracked aluminum plates using polymeric composite patches embedded with prestressed SMA wires. *Journal of Composite Materials*, 00219983231184441.
- Rebai, B., Mansouri, K., Chitour, M., Berkia, A., Messas, T., Khadraoui, F., & Litouche, B. (2023). Effect of Idealization Models on Deflection of Functionally Graded Material (FGM) Plate.
- Shinde, H., Kumar, P., Karnik, M., & Sonawane, N. (2023). Numerical simulation of pre-cracked thin aluminum alloy skin repaired with a FRP patch: Pre-crack length studies. *Materials Today: Proceedings*, 72, 1774-1779.
- Shinde, H., Kumar, P., Karnik, M., Shinde, P., & Todkar, A. (2020). Fatigue analysis of pre-cracked aluminium alloy thin sheets repaired with a CFRP patch at elevated temperature. *Journal of the Institution of Engineers (India): Series C*, 101, 303-311.
- Yousefi, A., Jolaiy, S., Hedayati, R., Serjouei, A., & Bodaghi, M. (2021). Fatigue life improvement of cracked aluminum 6061-T6 plates repaired by composite patches. *Materials*, 14(6), 1421.



© 2024 by the authors; licensee Growing Science, Canada. This is an open access article distributed under the terms and conditions of the Creative Commons Attribution (CC-BY) license (<http://creativecommons.org/licenses/by/4.0/>).